















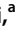





A New Phenotype in *Candida*-Epithelial Cell Interaction Distinguishes Colonization- versus Vulvovaginal Candidiasis-Associated Strains

 Arianna Sala,^a  Andrea Ardizzoni,^a  Luca Spaggiari,^b  Nikhil Vaidya,^c  Jane van der Schaaf,^c  Cosmeri Rizzato,^d  Claudio Cermelli,^a  Selene Mogavero,^e  Thomas Krüger,^f  Maximilian Himmel,^g  Olaf Kniemeyer,^f  Axel A. Brakhage,^f  Benjamin L. King,^{c,9}  Antonella Lupetti,^d  Manola Comar,^{h,i}  Francesco de Seta,^{h,i}  Arianna Tavanti,^j  Elisabetta Blasi,^a  Robert T. Wheeler,^{c,9}  Eva Pericolini^a

^aDepartment of Surgical, Medical, Dental and Morphological Sciences with Interest in Transplant, Oncological and Regenerative Medicine, University of Modena and Reggio Emilia, Modena, Italy

^bClinical and Experimental Medicine PhD Program, University of Modena and Reggio Emilia, Modena, Italy

^cDepartment of Molecular and Biomedical Sciences, University of Maine, Orono, Maine, USA

^dDepartment of Translational Research and of New Technologies in Medicine and Surgery, University of Pisa, Pisa, Italy

^eDepartment of Microbial Pathogenicity Mechanisms, Leibniz Institute for Natural Product Research and Infection Biology-Hans Knöll Institute (HKI), Jena, Germany

^fDepartment of Molecular and Applied Microbiology, Leibniz Institute for Natural Product Research and Infection Biology-Hans Knöll Institute (HKI), Jena, Germany

^gGraduate School of Biomedical Sciences and Engineering, University of Maine, Orono, Maine, USA

^hInstitute for Maternal and Child Health—IRCCS Burlo Garofolo, Trieste, Italy

ⁱDepartment of Medical, Surgical and Health Sciences, University of Trieste, Trieste, Italy

^jDepartment of Biology, University of Pisa, Pisa, Italy

ABSTRACT Vulvovaginal candidiasis (VVC) affects nearly 3/4 of women during their lifetime, and its symptoms seriously reduce quality of life. Although *Candida albicans* is a common commensal, it is unknown if VVC results from a switch from a commensal to pathogenic state, if only some strains can cause VVC, and/or if there is displacement of commensal strains with more pathogenic strains. We studied a set of VVC and colonizing *C. albicans* strains to identify consistent *in vitro* phenotypes associated with one group or the other. We find that the strains do not differ in overall genetic profile or behavior in culture media (i.e., multilocus sequence type [MLST] profile, rate of growth, and filamentation), but they show strikingly different behaviors during their interactions with vaginal epithelial cells. Epithelial infections with VVC-derived strains yielded stronger fungal proliferation and shedding of fungi and epithelial cells. Transcriptome sequencing (RNA-seq) analysis of representative epithelial cell infections with selected pathogenic or commensal isolates identified several differentially activated epithelial signaling pathways, including the integrin, ferroptosis, and type I interferon pathways; the latter has been implicated in damage protection. Strikingly, inhibition of type I interferon signaling selectively increases fungal shedding of strains in the colonizing cohort, suggesting that increased shedding correlates with lower interferon pathway activation. These data suggest that VVC strains may intrinsically have enhanced pathogenic potential via differential elicitation of epithelial responses, including the type I interferon pathway. Therefore, it may eventually be possible to evaluate pathogenic potential *in vitro* to refine VVC diagnosis.

IMPORTANCE Despite a high incidence of VVC, we still have a poor understanding of this female-specific disease whose negative impact on women's quality of life has become a public health issue. It is not yet possible to determine by genotype or laboratory phenotype if a given *Candida albicans* strain is more or less likely to cause VVC. Here, we show that *Candida* strains causing VVC induce more fungal shedding from epithelial cells than strains from healthy women. This effect is also accompanied by increased epithelial cell detachment and differential activation of the type I interferon

Editor Joseph Heitman, Duke University

Copyright © 2023 Sala et al. This is an open-access article distributed under the terms of the [Creative Commons Attribution 4.0 International license](https://creativecommons.org/licenses/by/4.0/).

Address correspondence to Robert T. Wheeler, robert.wheeler1@maine.edu, or Eva Pericolini, eva.pericolini@unimore.it.

The authors declare no conflict of interest.

[This article was published on 1 March 2023 with information missing from Acknowledgments. The Acknowledgments were corrected in the current version, posted on 4 April 2023.]

Received 18 January 2023

Accepted 9 February 2023

Published 1 March 2023

pathway. These distinguishing phenotypes suggest it may be possible to evaluate the VVC pathogenic potential of fungal isolates. This would permit more targeted antifungal treatments to spare commensals and could allow for displacement of pathogenic strains with nonpathogenic colonizers. We expect these new assays to provide a more targeted tool for identifying fungal virulence factors and epithelial responses that control fungal vaginitis.

KEYWORDS *Candida albicans*, epithelial cells, host-pathogen interactions, interferons, vulvovaginal candidiasis

Candida albicans is an opportunistic fungus that resides commensally in the vaginal tract of healthy women together with beneficial microbes, such as lactobacilli, and/or potential pathogens, such as *Gardnerella vaginalis* and group B *Streptococcus* (1, 2). Given the right circumstances, *C. albicans* is also able to cause acute and recurrent vulvovaginal candidiasis (VVC). VVC is a very common pathology, affecting 70 to 75% of women of child-bearing age at least once in their lifetime (3, 4). About 5 to 8% of these women will suffer from the recurrent form (RVVC), defined as the occurrence of at least four episodes of the acute form every year, requiring continual antifungal therapy (5, 6). Clinical signs of VVC include itching, burning, pain, and redness of the vaginal mucosa, often accompanied by vaginal white discharge, with a drastic reduction in the quality of life and mental well-being of women who are affected by this pathology. Moreover, VVC has been linked to a reduction in fertility (7, 8). Some host conditions have been implicated in VVC onset, although few factors have been associated with higher risk in multiple studies (1, 9–12). In addition, although some fungal traits are required in murine infection models, it is still not clear what induces *C. albicans* to switch from a harmless commensal to a virulent pathogen that triggers the onset of human VVC infection symptoms.

The current data suggest that in healthy subjects, *C. albicans* is tolerated in low numbers as a predominantly yeast-form commensal on the mucosal surface without triggering an epithelial immune response (1, 13). When local defense mechanisms are dampened, both *C. albicans* burden and virulence increase, and this may exceed the tolerance threshold of epithelial cells. This may occur due to estrogen-dependent fungal immune evasion (14). As the host responds and the fungus triggers an intense inflammatory response, this leads to proinflammatory cytokine release (such as interleukin-1 β [IL-1 β] and IL-6) and recruitment of nonprotective neutrophils (1, 12, 13, 15, 16). Several components have been implicated in the *in vitro* vaginal epithelial response to *C. albicans*, including upregulation of type I interferon (IFN), changes in many metabolic pathways, enhanced mitochondrial damage, activation of platelet-derived growth factor (PDGF) BB and NEDD9 pathways, and NLRP3 inflammasome activation (12, 17, 18).

Our previous work analyzing samples directly from women showed that there is a strong bias toward hyphal morphology and β -glucan exposure in fungi isolated directly from VVC patients compared to those from colonized women (19). However, it is unknown if this is driven by intrinsic fungal factors and/or host-associated traits. Studies in murine models suggest that there are strain-specific differences in the ability of clinical *C. albicans* isolates to cause disseminated disease (20), intestinal tract colonization (21–23), oropharyngeal thrush (24, 25), and vulvovaginal infection (26, 27). In addition to variation in VVC virulence, significant heterogeneity in filamentous growth, biofilm formation, candidalysin production, macrophage interaction, and other phenotypes has been described for VVC strains (26, 28–32). Several *C. albicans* genes have been implicated in inducing inflammation in murine VVC models, including those controlling *in vitro* hyphal growth and production of the candidalysin toxin and secretory aspartyl proteinases (SAPs) (26, 33–35). However, these phenotypes of filamentous growth, biofilm formation, candidalysin production, and SAP expression are found equally in VVC and colonizing strains, which is inconsistent with the idea that any of these easily measured *in vitro* phenotypes is a

primary driver of virulence in human infection. Thus, despite years of work it has not yet been possible to identify any *in vitro* phenotypes or disease-causing traits in *C. albicans* that correlate with human VVC as opposed to asymptomatic colonization. We hypothesized that any VVC virulence trait should be more common in isolates from VVC patients, although present in a subset of isolates from asymptomatic women that are capable of causing disease in the context of the right host environmental perturbation.

Here, we measured both intrinsic fungal traits and fungal traits revealed upon interaction with the host to identify virulence traits associated with symptomatic VVC. We found that the strains do not differ in overall genetic profile or behavior in culture media (i.e., multilocus sequence type [MLST] profile, rate of growth, and filamentation), but they have strikingly divergent behaviors when interacting with vaginal epithelial cells. Specifically, VVC pathogenic isolates grow more prolifically and are shed more from epithelial cells than colonization isolates. Transcriptome sequencing (RNA-seq) analysis of vaginal epithelial cell challenges with a selected VVC strain and colonizing strain revealed many differentially regulated pathways, including the type I interferon, integrin, and ferroptosis pathways. Of particular interest, the type I interferon pathway is activated more by the colonizing strain, and we find that blocking its activity limits strain-specific fungal shedding. Taken together, these data suggest that VVC strains may intrinsically have greater pathogenic potential via differential elicitation of epithelial responses, including through the type I interferon pathway. Therefore, it may be possible to evaluate the pathogenic potential of *Candida* isolates *in vitro* to refine diagnoses and more readily determine if *C. albicans* is the likely agent for vaginitis symptoms or a harmless commensal.

RESULTS

VVC strains do not group phylogenetically. To date, it has not been possible to categorize *C. albicans* strains as “VVC pathogenic” versus “colonizing” through correlation of *in vitro* pathogenic phenotypes with strains originating from VVC. Here, we tested the hypothesis that some *C. albicans* strains have virulence traits that make them intrinsically more likely to cause symptomatic VVC in healthy women: VVC pathogenic. We took a mixed set of strains that had been directly characterized from vaginal swabs for morphology and cell wall epitope unmasking (19). This study and others have demonstrated that fungi actively causing VVC tend to be in hyphal form, whereas those from asymptomatic women tend to be in yeast form when examined directly in vaginal swabs. We first tested if any *C. albicans* clades are more associated with VVC by MLST analysis. MLST analysis was performed according to established protocols and did not reveal any genetic clustering distinguishing strains causing VVC versus those involved in colonization (Fig. 1). *C. albicans* isolates fell into different clades (with a majority of clade I strains [data not shown]).

VVC strains do not group based on candidalysin allele or expression. It has been recently shown that candidalysin, a *C. albicans* hypha-associated toxin, is important for inducing an inflammatory signal in a murine VVC model, suggesting a potentially pathogenic role during VVC (36). Furthermore, the two main types of candidalysin alleles in clinical isolates (SC5314- or 529L-like) have quite different abilities to elicit inflammation in the murine model of VVC (26). Clinical VVC isolates have either the SC5314 or 529L allele of candidalysin in approximately even ratios, raising the question of whether these allelic differences are important for VVC pathogenesis in humans (26). We sought to test, in our collection of clinical *Candida* strains, whether there was any association between candidalysin genotype or expression and symptomatic VVC. The candidalysin-encoding region of *ECE1* was amplified from each isolate, and the DNA sequences of alleles from individual isolates were aligned. Many strains (8/16 at the DNA level and 6/16 at the amino acid level) were found to be heterozygous at the *ECE1* locus in the region encoding candidalysin, although even those heterozygous strains had very similar candidalysin sequences for both alleles at both the DNA (>87% identity) and predicted protein (>89% identity) levels (Fig. 2). All but one of the alleles grouped with the SC5314 sequence, while the outlier grouped with

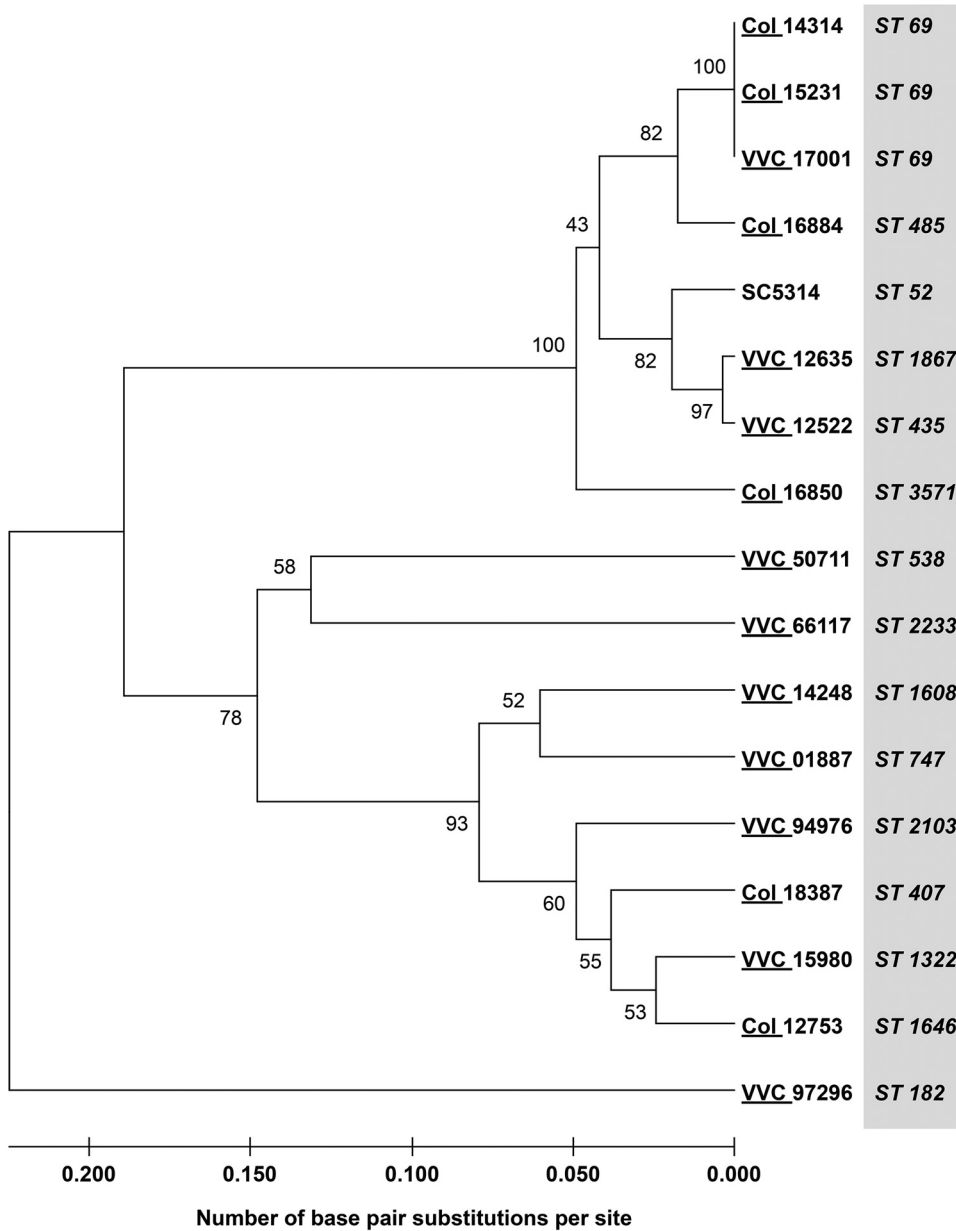


FIG 1 Unrooted neighbor-joining tree showing *p*-distance for *C. albicans* clinical isolates typed by MLST, using SC5314 as reference strain. The number for each cluster node indicates the bootstrap value. Bootstrapping was set at 500.

the 529L sequence (Fig. 2A; see Fig. S1 in the supplemental material). Interestingly, the relationships according to MLST (Fig. 1) did not correspond well to the relationships according to candidalysin *ECE1* sequences (Fig. 2). Accordingly, in this set of clinical isolates there was no association between candidalysin sequence and symptomatic VVC infection (Fig. 2).

Since candidalysin genotype is only one indicator of expression and function, it remains possible that mRNA or protein expression levels of mature candidalysin distinguish colonizing from symptom-inducing strains. Therefore, we measured secreted candidalysin levels from each strain growing *in vitro* under strong hypha-inducing conditions by liquid chromatography-tandem mass spectrometry (LC-MS/MS) as previously described (37). Three clinical isolates (66117, 94976, and 50711) produced detectable levels of candidalysin, but most of the strains failed to produce sufficient levels of candidalysin for detection (indicated by # in Fig. 2B; Data Set S1). There was no significant correlation between lack

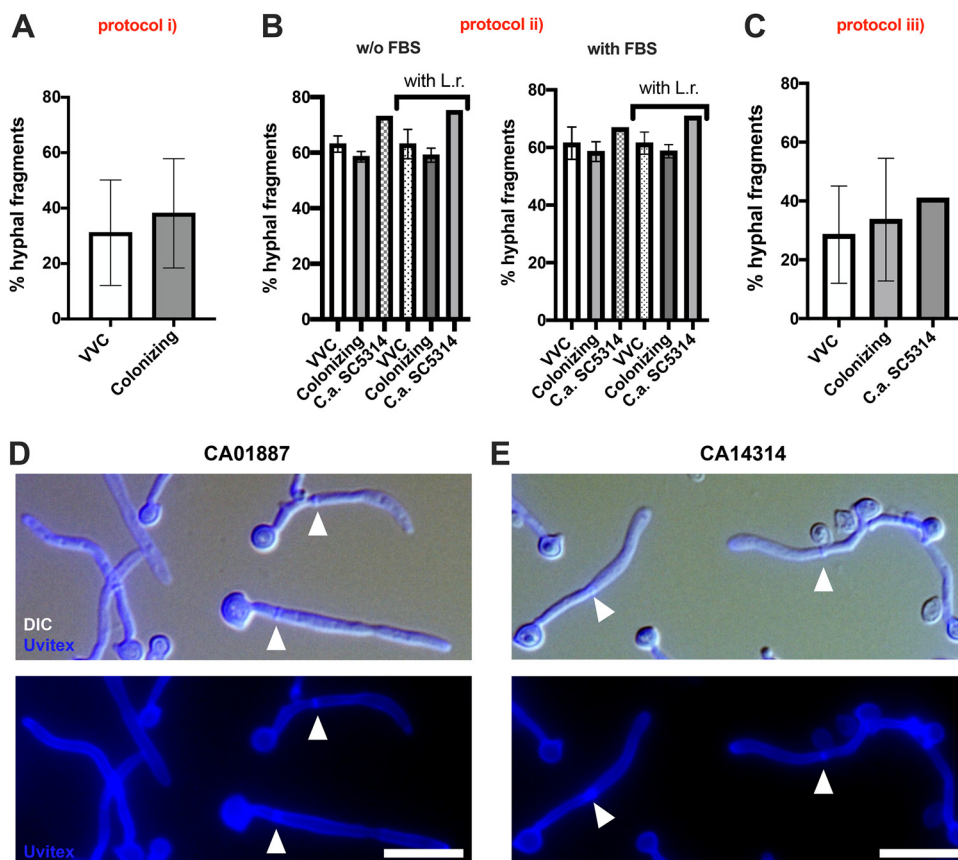


FIG 3 *C. albicans* hyphal fragment production. Data in the graphs show the mean percentage \pm standard deviation (SD) of hyphal fragments produced by VVC and colonizing *C. albicans* strains after 24 h of culture in RPMI 1640 (protocol i) (A), in RPMI or RPMI plus 10% FCS in the presence or absence of *Lactobacillus rhamnosus* (L.r.) (protocol ii) (B), or during infection of a monolayer of A431 cells (protocol iii) (C). Statistical analysis was performed according to Student's *t* test (A and C) and Kruskal-Wallis test, followed by Dunn's multiple-comparison test or one-way ANOVA, followed by Tukey's multiple-comparison test (left and right graphs of panel B, respectively). Panels D and E show representative images of hyphal segments from the 01887 (D) and 14314 (E) strains from experimental protocol ii, grown in sgRPMI. Arrowheads indicate the septa separating one hyphal segment from another. The data come from at least 3 biological replicates.

time, although different growth rates may have occurred, no differences in overall growth were found after culture for 24 h in YPD broth (Fig. S2A). These results suggest that each of these strains is able to make sufficient hyphae in tissue culture medium to be pathogenic and that unidentified environmental factors in the host may play a large role in limiting filamentous growth during colonization as opposed to infection.

Since vaginal epithelial cells can influence *C. albicans* growth *in vitro* (43), we examined if differences in filamentation between these two groups of isolates were associated with interaction with host cells. We challenged A431 vaginal cells for 24 h with *C. albicans* strains and then measured the propensity of *C. albicans* strains to form hyphae (protocol iii). Again, no cohort-specific differences in the percentage of hyphal segments were observed (Fig. 3C; Table S1A in Data Set S2). Taken together, we found no differences in overall filamentation between cohorts of strains isolated from VVC or colonized women, even in the context of infection of the vaginal epithelium. This suggests that more complex host intrinsic mechanisms may play the most important role in regulation of filamentous growth and pathogenesis in human vaginal mucosa (1, 44).

VVC strains proliferate more and are shed more during epithelial infection. VVC is associated with inflammation, pain, and vaginal discharge (3, 4). We sought to translate these human disease symptoms into *in vitro* phenotypes and test for differences that might distinguish colonizing isolates from symptomatic isolates. First, we assessed the ability of each strain to damage vaginal epithelial cells, resulting in release of lactate dehydrogenase.

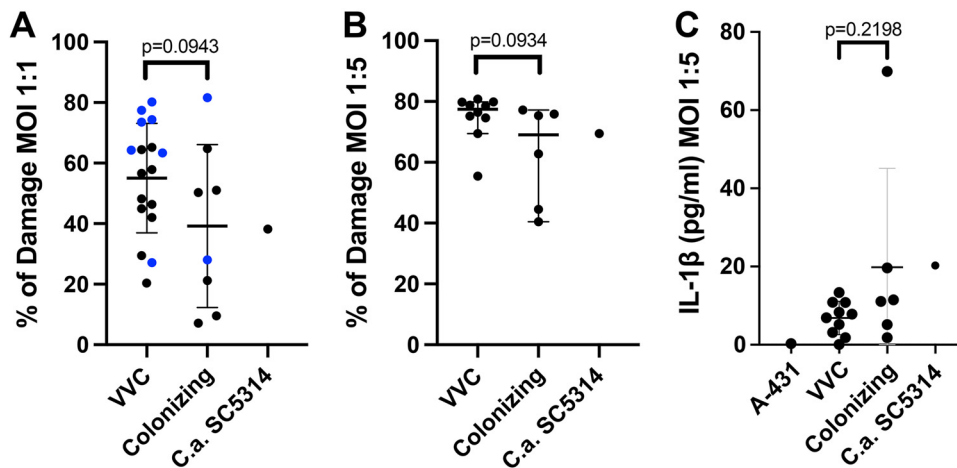


FIG 4 Vaginal epithelial cell damage and IL-1 β production. (A and B) Vaginal cell damage (LDH release) after 24 h of infection with VVC and colonizing *C. albicans* strains or by the reference strain SC5314 at an MOI of 1:1 (A) or 1:5 (B). The blue dots highlighted in panel A indicate results from an additional group of 9 isolates the provenance of which had been previously reported (see reference 44). (A) Mean \pm SD of each cohort; (B) median of each cohort with 95% confidence interval (CI). Each data point represents the average from three biological replicates. (C) IL-1 β (picograms per milliliter) released by vaginal cells after 24 h of infection with VVC and colonizing *C. albicans* strains or by the reference strain SC5314 at an MOI of 1:5; (C) mean \pm SD of each cohort. Each data point represents the average from 4 biological replicate experiments. Statistical analysis was performed according to unpaired Student's *t* test (A; MOI of 1:1) and Mann-Whitney test (B and C; MOI of 1:5), according to data normality. *P* values of >0.05 were considered not significant and are shown above the data.

We challenged a monolayer of A431 cells with each *C. albicans* isolate and measured lactate dehydrogenase (LDH) release. Here, we observed no significant difference in LDH release provoked by VVC versus colonizing strains. Nonetheless, there was a weak trend toward reduced epithelial damage caused by colonizing strains (irrespective of the multiplicity of infection [MOI] used), compared to VVC pathogenic strains (Fig. 4A and B). Interestingly, this trend holds for an independent set of mixed pathogenic/colonizing isolates from vaginal swabs described by Ardizzoni et al. (44) (blue dots in Fig. 4A).

Next, we assayed epithelial cell-produced inflammatory signals. It is known that IL-1 β and polymorphonuclear leukocyte (PMN) recruitment are associated with symptomatic inflammation characteristic of VVC in humans (19, 39, 45). We measured levels of a suite of secreted inflammatory factors and found overall low elicitation from A431 cells, similar to what has been reported (36, 46). While some IL-1 β was produced by epithelial cells upon *C. albicans* challenge, IL-1 β levels in cell culture supernatants were not significantly different between strains from VVC versus colonized women (Fig. 4C).

Finally, we sought an *in vitro* technique to approximate the process leading to vaginal discharge, which contains epithelial cells and associated microbes being shed into the vaginal lumen (47). To maintain tissue homeostasis, the vaginal epithelium induces shedding of mature superficial epithelial cells, while the renewal of cells conserves barrier integrity (48, 49). Bacterial infection can induce the exfoliation of epithelial cells (50–53). *C. albicans* is shed in association with host cells, providing a potential mechanism for elimination of invading hyphae but also potentially damaging the epithelium (54).

We employed two similar experimental protocols to measure the level of *C. albicans* shed from an infected epithelium. First, we used the shedding protocol described by Graf et al. (54) to quantify the total level of *C. albicans* shed in the supernatants (shed cells in suspension, as shown by the blue fraction in Fig. 5A) and the live *C. albicans* cells associated with the epithelium (exfoliated and loosely adherent cells, as shown by the yellow fraction in Fig. 5A, plus adherent cells, as shown by the green fraction in Fig. 5A). The cell types and measurements of this shedding protocol are summarized in the upper part of Fig. 5A. We measured overall fungal growth on vaginal epithelia (all cells) and found a trend that VVC strains proliferate more robustly than colonizing strains ($P = 0.0559$) (Fig. 5B). We then measured shedding and found a significantly

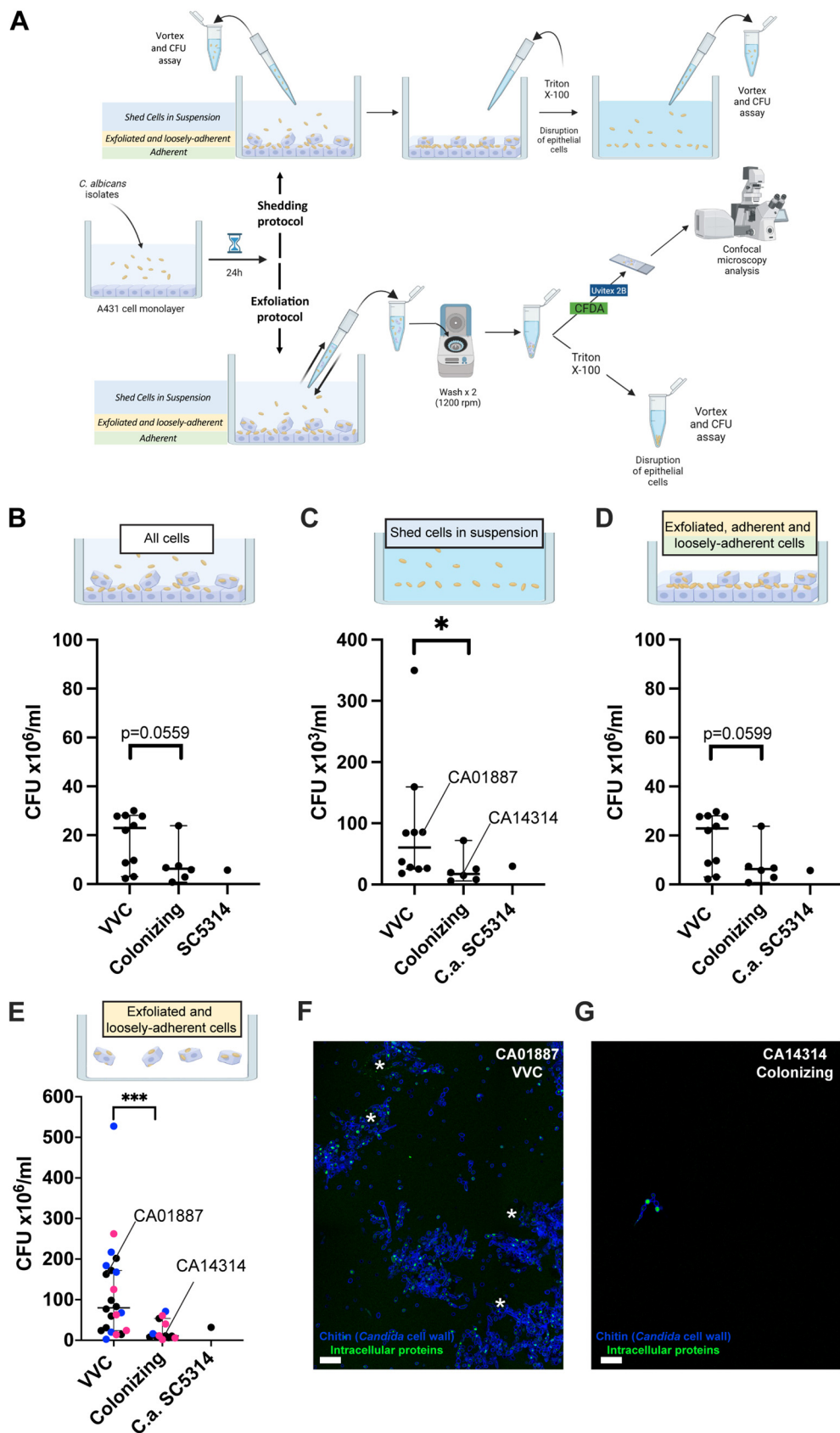


FIG 5 *C. albicans* shedding from vaginal epithelium. (A) Shedding of epithelial and fungal cells was measured by either the shedding protocol (A, upper) or the exfoliation protocol (A, lower). Epithelial or fungal cells could be (Continued on next page)

higher number of CFU in supernatants from challenges with VVC *C. albicans* strains than in those with colonizing isolates (Fig. 5C; shed cells in suspension; $P = 0.0110$). In contrast, no significant differences were observed in the level of *C. albicans* attached to the epithelium between strains from the VVC versus colonizing group (Fig. 5D; exfoliated, adherent, and loosely adherent cells), although there was a trend toward fewer fungal cells in the colonizing strain cohort ($P = 0.0599$). Unfortunately, this protocol does not examine if epithelial cells remain adherent or exfoliate from the substrate, nor does it quantify fungal cells associated with exfoliated epithelial cells.

To measure the level of *Candida* associated with nonadherent/exfoliated epithelial cells, we developed the exfoliation protocol (summarized in the lower part of Fig. 5A). By gently pipetting off nonadherent epithelial and fungal cells from the epithelial monolayer, we were able to measure live *C. albicans* cells that were either nonadherent or were shed in association with exfoliated epithelium (exfoliated and loosely adherent cells, shown as yellow and green in Fig. 5A). Similar to the shedding protocol, we also found significantly higher levels of fungal shedding in challenges with VVC versus colonizing strains ($P = 0.0003$) (Fig. 5E; exfoliated and loosely adherent cells). Confocal microscopy analysis of supernatants from representative VVC (CA01887) and colonizing (CA14314) strains revealed a correspondingly higher level of epithelial cells shed in association with live *Candida* after CA01887 infection than in the CA14314 strain infection (Fig. 5F to G). Interestingly, shed fungal cells in VVC isolate challenges were often found associated with vaginal epithelial cells (marked with asterisks), suggesting that the fungal shedding could be due to exfoliation of epithelial cells. To determine if differential adhesion to plastic accounted for any cohort-specific differences in shedding, the assay was carried out without any preaddition of epithelial cells. There was no overall difference in plastic adhesion between cohorts of isolates, suggesting that shedding differences are not mediated by fungus-plastic interaction (Fig. S2B). Taken together, these complementary results suggest that the VVC-associated isolates induce more shedding of *Candida* and exfoliation of epithelial cells than colonization-associated isolates. This is consistent with the idea that these VVC-associated strains induce more vaginal discharge in women, leading to symptomatic disease.

Differential epithelial response to VVC versus colonizing strain. To discover the reasons for this differential behavior of *C. albicans* isolates in the shedding process, we looked more carefully at epithelial responses to the two classes of *C. albicans* strains, performing RNA-seq analysis. We challenged a monolayer of A431 vaginal epithelial cells with a representative VVC strain or a colonizing strain (i.e., CA01887 and CA14314, respectively [data on these strains are shown in Fig. 5]) and isolated RNA from the infected cells. Several different human signaling pathways were significantly associated with *C. albicans* challenge for each of the two strains, based on Ingenuity Pathway Analysis (IPA) (Fig. S3 and Data Set S3). However, there were also pathways with divergent activation upon infection with VVC and colonizing strains, including the type I

FIG 5 Legend (Continued)

attached to the substrate, loosely attached to the substrate, or shed in suspension. Each protocol measures different fractions of the total challenge, as indicated by the workflow. The shedding protocol measures shed cells in suspension (top panels), whereas the exfoliation protocol measures shed cells bound to exfoliated cells and/or loosely associated with the epithelium (bottom panels). (B to G) Data in the graphs show the mean \pm SD CFU from 3 different experiments after 24 h of infection of the vaginal epithelial monolayer with the indicated *C. albicans* strains at an MOI of 1:1. (B to D) Shedding protocol. (B) Overall *C. albicans* CFU for each infection (all cells); (C) *C. albicans* CFU shed in the supernatants (shed cells in suspension), and (D) *C. albicans* CFU attached to or loosely associated with vaginal epithelium (exfoliated, adherent, and loosely adherent cells). (E to G) Exfoliation protocol. (E) *C. albicans* CFU shed in supernatant in association with shed epithelial cells (exfoliated and loosely adherent cells). In panel E, the black dots represent the standard 16 clinical strains used throughout the study, blue dots indicate an additional group of 9 isolates tested (see reference 44), and magenta dots indicate a third group of 10 isolates from women with RVVC or healthy colonized women obtained from IRCSS Burlo Garofolo Trieste, Italy. Statistical analysis was performed according to the Mann-Whitney test. P values of <0.05 (*) and <0.001 (***) were considered significant. P values of >0.05 are not considered significant and are shown above the data. Panels F and G show representative images of *C. albicans* shedding of the VVC strain CA01887 (F) and the colonizing strain CA14314 (G). Exfoliated and loosely adherent cells are shown, including epithelial cells with punctate CFDA in the cytoplasm (marked by asterisks) and *Candida* cells (blue with bright dots of CFDA staining). Scale bar = 20 μ m.

interferon (Fig. 6A), integrin (Fig. 6B), and ferroptosis pathways (Fig. 6C; Table S1B in Data Set S2) signaling pathways. These three pathways were selected for more detailed IPA analysis due to published links between the pathways and pathogen challenge or infection (52, 53, 55–62). More detailed analysis of pathways indicated that the VVC-associated strain evoked a weaker type I IFN and ferroptosis pathway induction but a stronger integrin pathway activation. Gene Ontology (GO) enrichment analysis identified hypoxia signaling as regulated in both infections, which is a GO biological process term previously identified by transcriptomic analysis of *Candida*-A431 challenges (63) (Data Set S4). While the roles of hypoxia, integrin signaling, and ferroptosis were not investigated further, we went on to functionally test the role of type I interferon signaling in fungal shedding because of its known role in A431 epithelial response to *C. albicans*.

Differential type I interferon pathway activation functionally linked to shedding difference. Lower type I interferon pathway induction suggested the possibility that VVC-causing *C. albicans* strains do not elicit type I interferon when interacting with the host vaginal mucosa, preventing a protective response and allowing greater damage (63). A prediction of this idea is that inhibition of the IFN- α/β receptor (IFNAR) would increase shedding only during challenges with the colonizing strain CA14314. To test this, we used a neutralizing anti-IFNAR antibody and measured shedding with either the colonizing or pathogenic strain (using the shedding protocol). In agreement with this hypothesis, blocking the IFNAR led to significantly increased *C. albicans* shedding of the colonizing strain but not of the VVC pathogenic strain (Fig. 6D, red dots), while this intervention had no significant effect on the number of viable adherent or total *Candida* cells for either infection (Fig. 6E and F, red dots). By extending these experiments to assay several additional strains, we found overall that the shedding of colonizing strains has greater dependence on IFNAR as opposed to that of the VVC strains, although there is significant heterogeneity in both cohorts (Fig. 6D). Again, IFNAR blockade did not affect viable adherent or total numbers of *Candida* cells (Fig. 6E and F).

DISCUSSION

Despite decades of work on *in vitro* characterization of vaginal clinical isolates of *C. albicans*, it has not been possible to attribute any pathogenesis-associated phenotypes that distinguish VVC pathogenic strains from those associated with asymptomatic colonization. This negative evidence has led to a focus on host-specific differences in response to fungi in the vaginal mucosa (1, 12, 13). In contrast, our results distinguish a cohort of VVC isolates from their colonizing counterparts using phenotypes revealed only upon their interaction with vaginal epithelial cells. These data suggest that VVC pathogenic strains are better able to proliferate during epithelial challenge and are shed more efficiently with epithelial cells. These phenotypes are consistent with the frequent presence of white vaginal discharge in VVC, which contains epithelial and fungal cells.

As predicted by the host-microbe damage response framework (13), there are likely both host- and *Candida*-associated conditions that combine to result in an outcome of colonization or symptomatic VVC. Our combined RNA-seq–IFNAR inhibition results with two representative isolates suggest that some colonizing strains may preferentially induce type I interferon, which then aids in epithelial defense and limits shedding and exfoliation. This suggests that VVC pathogenic strains may have the ability to avoid eliciting type I interferon pathway activation and thereby block this protective response in epithelial cells. Type I interferon has not been previously implicated in human VVC by genome-wide association analysis, but recombinant interferon beta has some protective effects in a rat VVC model and type I interferon is present in vaginal fluid of VVC patients (64, 65). Recent work suggests that the *C. albicans* SC5314 activates the epithelial interferon pathway through the candidalysin toxin, which is linked to mitochondrial damage (63). No secreted candidalysin was detected from either of the strains used in our RNA-seq experiments, although it may be present at higher levels in the invasion pocket during infection (66). While *ECE1* allelic differences are associated with inflammation in murine VVC (26), we found no association between the *ECE1* allele and VVC, suggesting the possibility that candidalysin is

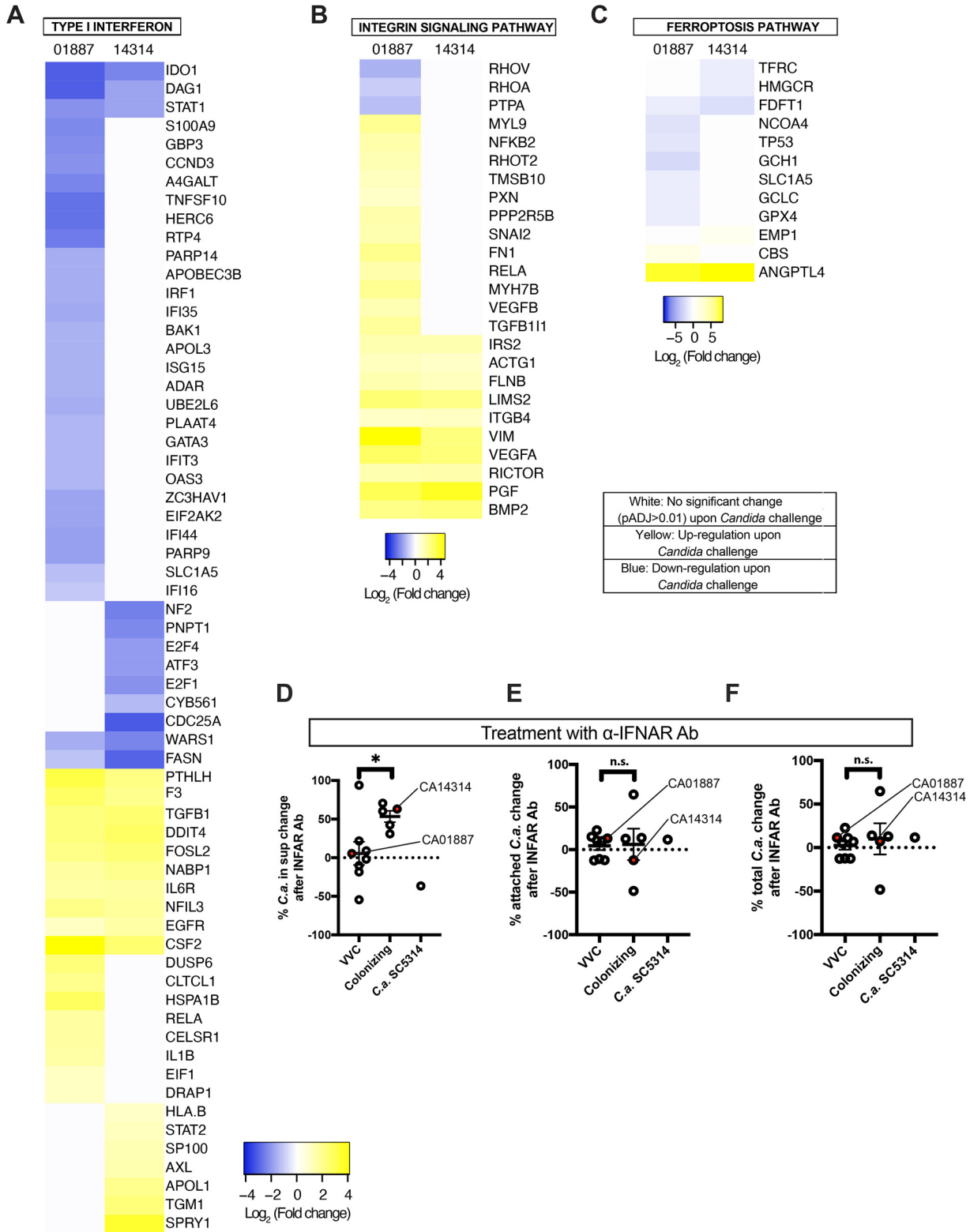


FIG 6 CA01887 and CA14314 differentially activate type I interferon, integrin, and ferroptosis pathways. A431 vaginal epithelial cells were challenged with either CA01887 or CA14314 for 24 h. Differential RNA-seq was performed on two biological replicates of mock-infected versus infected challenges and analyzed with DESeq2 and Ingenuity Pathway Analysis. (A to C) Differentially regulated genes from three pathways with divergent responses upon *C. albicans* challenge are shown with statistically significant upregulation (yellow), significant downregulation (blue), or no significant change (white). The range for each is shown below (values are the log₂ ratio of fungal challenge to mock challenge). The cutoff for significant changes was an adjusted *P* value (*P*_{adj}) of <0.01. (D to F) Summary of IFNAR inhibition of shedding for several VVC and colonizing strains. Shown is the mean percentage of change ± SD in CFU from at least 3 different experiments after 24 h of infection of the (Continued on next page)

more important for different classes of strains (VVC versus colonizing) and/or is more important for murine than human VVC (38).

In addition to differential regulation of type I interferon signaling, IPA identified many other pathways that are differentially induced by the VVC pathogenic strain. One pathway activated only by the VVC strain is the integrin signaling pathway, which is targeted by at least two bacterial pathogens of the vaginal tract: group B *Streptococcus* and *Neisseria gonorrhoeae* (52, 53). *C. albicans* encodes proteins that engage with integrins, in addition to having an integrin-like cell wall protein of its own (56–58, 60, 61, 67). Another pathway predicted to be activated preferentially by the colonizing strain was the ferroptosis pathway, a cell death pathway that is also targeted by bacterial pathogens (55, 59, 62). Intriguingly, iron chelators reduce *C. albicans* virulence in both oral and vaginal murine disease models, although this might be attributable to a direct antifungal effect as well (68, 69). To date, there have been no reports of either integrin or ferroptotic signaling being involved in VVC, although recent work implicates immune cell ferroptosis in *Candida* virulence (70).

Vaginal isolates of *C. albicans* have been analyzed both genetically and phenotypically *in vitro* by many groups, although no clades have been linked to symptomatic VVC in multiple locations. These studies, together with the current report, indicate that *C. albicans* VVC isolates come from all clades and express heterogeneity with respect to biofilm production, macrophage interactions, and hyphal induction under different conditions (19, 26, 28–32). However, none of these phenotypes has been specifically linked to VVC strains versus colonizing strains in human disease.

Taken together, our data suggest that VVC strains may have more intrinsic pathogenic potential via differential elicitation of epithelial responses, including through the type I interferon pathway. Therefore, it may be possible to evaluate pathogenic potential by shedding and exfoliation *in vitro* to refine diagnoses and more readily determine if *C. albicans* is the likely agent for vaginitis symptoms. It is important to note that our strains from colonized and VVC individuals exhibit diverse levels of shedding with overlapping ranges, suggesting they are not homogeneous. It is likely that some strains isolated from non-symptomatic patients nevertheless have the ability to cause VVC under the right circumstances and thus should be considered “VVC” strains. Alternatively, some isolates from VVC patients with low shedding might be in mixed VVC infections with several *C. albicans* strains, including a more virulent strain whose colony was not picked by simple chance. Further longitudinal studies of strains from asymptomatic individuals and/or those with RVVC and further depth in sampling of multiple isolates may help to resolve these potential complicating factors.

It will be of particular interest to understand if “pathogenic” phenotypes are more likely to be associated with negative outcomes in pregnancy or in recurrent VVC (71). However, it is not yet clear if these differences are conserved among all VVC pathogenic and colonizing strains nor whether these epithelial transcriptional differences translate into functional divergence. Furthermore, there are many other *Candida* epithelial cell-interacting factors and other differentially regulated epithelial pathways that may be just as important but remain untested in the context of this phenotype that differentiates VVC pathogenic strains. It is possible that *in vitro* assays to determine the pathogenic potential of clinical isolates would permit more antifungal treatments targeted toward pathogenic rather than colonizing strains. Furthermore, such assays would provide tools for identifying fungal virulence factors and epithelial responses that may be decisive in the switch from commensal to pathogen. Discovery of the molecular mechanisms underlying this phenotypic difference will therefore be of particular interest going forward.

FIG 6 Legend (Continued)

vaginal epithelial monolayer with VVC or colonizing strains in the presence or absence of neutralizing IFNAR antibody (Ab). All experiments used the shedding protocol. (D) *C. albicans* CFU shed in the supernatants (cells in suspension); (E) *C. albicans* CFU attached to vaginal epithelium (exfoliated, adherent, and loosely adherent cells); (F) overall *C. albicans* CFU for each infection (all cells). Red dots indicate the strains CA01887 and CA14314, which were used in the original RNA-seq experiments. The statistical comparisons between VVC and colonizing strains were performed according to the unpaired Student's *t* test. *P* values of <0.05 (*) were considered significant. n.s., not significant (*P* > 0.05).

MATERIALS AND METHODS

Microbial strains and culture conditions. A total of 36 clinical *C. albicans* strains were employed in this study, in addition to the reference strain SC5314. The list of *C. albicans* clinical isolates is reported in Table S1C in Data Set S2 in the supplemental material. The core group of strains used throughout this study is a set of 16 clinical isolates obtained from women with VVC or healthy colonized women described by Pericolini et al. (19). All of the subjects were nondiabetic and were not taking antifungal therapeutics. Briefly, colonizing strains were obtained from women attending an obstetrics/gynecology clinic for routine screening, while VVC subjects had at least two diagnostic symptoms (vaginal discharge, itching, burning, or dyspareunia). None of the recruited women had RVVC. Further recruitment of subjects from the same populations yielded an additional group of 9 isolates from women with VVC ($n = 7$) or healthy colonized women ($n = 2$) that were used only for selected experiments and were initially described by Ardizzoni et al. (44). Details of the women from which these strains were obtained together with the ethics statements have been provided elsewhere (19, 44). A second cohort of isolates (project RC 13/18 ID Study 2715) was obtained through a different study at the IRCSS Burlo Garofolo of Trieste and collected from women with RVVC ($n = 5$) or healthy colonized ($n = 5$) women. Samples were obtained from asymptomatic women attending the gynecology clinic during screening programs or from women with a history of RVVC being seen for follow-up diagnosis and therapy. Details of these samples (screening for bacteria, hyphae, and neutrophils) are included in Table S1D in Data Set S2.

Fungal cultures were maintained by weekly passages onto Sabouraud dextrose agar (SDA) plates (Oxoid, Milan, Italy). The day before each experiment, fresh *Candida* cultures were seeded onto SDA plates or YPD (yeast extract-peptone-dextrose) broth according to the experimental protocol and incubated at 37°C. After overnight incubation, fungal cells were harvested by a sterile inoculating loop, suspended in phosphate-buffered saline (PBS) (EuroClone, Wetherby, United Kingdom), washed twice by centrifugation at 3,500 rpm for 10 min, counted with a Bürker chamber and suspended at the desired concentration in culture media different for every experiment (see below). The reference strain, *Lactobacillus rhamnosus* ATCC 7469, was maintained in frozen stocks at -80°C in tryptic soy broth (TSB) (Difco Laboratories, Detroit, MI, USA) with 5% (vol/vol) glycerol. Bacterial cultures were maintained by weekly passages onto De Man-Rogosa-Sharp (MRS) agar (Oxoid, Milan, Italy) plates.

Vaginal epithelium. The human A431 vaginal epithelial cell line, obtained from ATCC, was grown in Dulbecco's modified Eagle's medium (DMEM) plus 10% defined fetal bovine serum (FBS) (HyClone, Logan, UT, USA), gentamicin (50 mg/mL) (Bio Whittaker, Verviers, Belgium), ciprofloxacin (Ciproxin) (2 mg/mL) (ICN), and L-glutamine (2 mM) (EuroClone, Milan, Italy).

One day before the experiment, vaginal cells (4×10^5 /mL/well) in DMEM plus 5% FBS were seeded in a 24-well plate and incubated for 24 h at 37°C plus 5% CO_2 to allow the formation of a monolayer. For the quantification of *C. albicans* hyphal segment by protocol iii, cells were seeded in 8-well chamber slides.

MLST analysis. The isolates were tested by MLST as previously described (72, 73), using the consensus scheme available at <https://pubmlst.org/organisms/candida-albicans>. The ABC type (A, B, or C) and mating type-like (MTL) types (a/α , a/a , or α/α) were determined by PCR as previously described (74). Similarities between sequence data were analyzed in terms of p -distance with MEGA version 11 (75), and results with 500 bootstrap replications are depicted as a dendrogram by the unweighted-pair group method with arithmetic averages (UPGMA). The analyses were based on concatenated data from all known polymorphic sites, duplicated to allow the discrimination of homozygous and heterozygous differences (73).

ECE1 genotypic analysis. DNA was isolated from each strain by Smash & Grab (76) and was amplified with the forward primer 5'-ATCATCCACCATGCTCCAG-3' and either 251REV (5'-TTAGAGATAAGTCTTGGA GCATTAGC-3') or 255REV (5'-TTGTTGAACAGTTTCCAGGACG-3'). Primers were designed within the P2 and P4 regions in areas most highly conserved in the available *ECE1* sequences from GenBank. PCR fragments were directly sequenced by Sanger sequencing. For amplifications that gave scrambled sequence indicating frameshifts, PCR products were cloned into pGEM-T Easy (Promega), several clones were sequenced by Sanger sequencing, and two consensus alleles were constructed. In some cases, frameshifts were outside the CL-encoding sequence, so both alleles shared the same CL sequence. Sequences were trimmed and then aligned with Clustal Omega (77), followed by nearest-neighbor joining in Simple Phylogeny (78).

Quantification of *C. albicans* hyphal segments. (i) Protocol i. A loop of each *C. albicans* strain was grown for 18 h at 37°C in 10 mL of RPMI 1640 under rotation. Cells were washed and resuspended in 100 μL of PBS (EuroClone, Wetherby, United Kingdom) plus 1% bovine serum albumin (BSA) (Sigma-Aldrich). Once washed, calcofluor white (1:20 from 100 $\mu\text{g}/\text{mL}$ stock; Fluorescent Brightener 28 F3543) (Sigma-Aldrich) was added, and cells were incubated for 30 min on ice. Cells were washed three times and resuspended in 50 μL . A 10- μL aliquot was imaged with a Zeiss Axiobserver Z1 microscope and Axiocam MRm camera using DAPI (4',6-diamidino-2-phenylindole) filter, using a Plan Neofluor 40-by-0.75 numerical aperture (NA) air objective, and Zeiss Axiovision software. z-stacks were processed in ImageJ by creating maximum projections and then scored as follows. Morphology was scored by counting all elongated cells, either pseudohyphae or hyphae, as filamentous. Calcofluor white staining was used to identify septa and thus to identify individual filament segments in hyphae. Counts were pooled for all fields imaged of a given sample.

(ii) Protocol ii. The day before each experiment, fresh *Candida* cultures were seeded onto SDA plates and incubated overnight at 37°C. Cells were harvested by a sterile inoculating loop, washed in PBS, and suspended at 4×10^6 yeast cells/mL. The suspension was then divided into 3 aliquots, each of them was washed again, and the pellets were resuspended in PBS, in gRPMI (i.e., RPMI 1640 [Gibco, Grand Island, NY, USA] with 2 mM L-glutamine [EuroClone, Milan, Italy]) or in sRPMI (i.e., RPMI 1640 with 2 mM L-glutamine and 10% defined FBS [Defined HyClone, Logan, UT, USA]). The day before each experiment, fresh *L. rhamnosus* cultures were seeded onto MRS plates and incubated overnight at 37°C in anaerobic conditions. Bacteria were harvested by a sterile inoculating loop, suspended in TSB, and

washed with PBS. The bacterial concentration was calculated by interpolating optical density (OD) values to a stored *Lactobacillus* standard curve, which had been previously set up in our laboratory. The bacterial concentration was adjusted to 4×10^7 lactobacilli/mL and divided into 2 aliquots. Each aliquot was pelleted and resuspended in gRPMI and sgRPMI. A combination of 100 μ L of *C. albicans* suspension with or without *L. rhamnosus* in gRPMI or sgRPMI was then seeded in a Lab-Tek II chamber slide (Nalge Nunc International, Naperville, IL, USA). The chamber slide was incubated at 37°C with 5% CO₂ for 3 h. At 15 min before the end of the incubation, 40 μ L of 1% Uvitex 2B fluorescent dye (Polysciences, Inc., PA, USA) was added to each well. All the wells were then washed twice (5 min each) with gRPMI or sgRPMI (all kept at 37°C) and fixed for 30 min with 4% paraformaldehyde (PFA) (Sigma-Aldrich) in PBS at +4°C. The slides were then washed twice with cold PBS (10 min each). The chamber walls were removed, and the slide surface was treated with ProLong Gold antifade reagent (Molecular probes, Invitrogen, St. Louis, MO, USA). The cells were imaged by epifluorescence microscopy Nikon Eclipse 90i (Nikon Instruments, Tokyo, Japan). Five fields/well/experimental condition were imaged and counted for morphology, as described for protocol i. Hyphal segments were counted considering the septa separating one hyphal segment from another. Only fields containing a total number of fungi ranging between 50 and 200 were chosen.

(iii) Protocol iii. One hundred microliters of each *C. albicans* strain suspension was seeded in the wells of Lab-Tek II chamber slides containing a monolayer of A431 cells in DMEM plus 5% FBS. The chamber slide was incubated at 37°C with 5% CO₂ for 24 h. After incubation, 40 μ L of 1% Uvitex 2B was added to each well and the chamber slide was placed again at 37°C with 5% CO₂ for a further 15 min. At the end of the incubation, all the wells were washed, fixed, and imaged by epifluorescence microscopy. Five fields/well/experimental condition were imaged and counted for morphology as described for protocol i. Only fields containing a total number of fungi ranging between 50 and 200 were chosen.

Candidalysin proteomics. Strains were grown in yeast nitrogen base (YNB) medium containing 2% sucrose, 75 mM 3-N-morpholinopropanesulfonic acid (MOPS) buffer (pH 7.2), and 5 mM *N*-acetyl-D-glucosamine at 37°C. After solid-phase extraction of hyphal supernatants, the resulting concentrated peptides were analyzed as described previously (37). Briefly, dried peptides were resolubilized in 100 μ L of 0.2% HCOOH in 71:27:2 (vol/vol/vol) acetonitrile (ACN)-H₂O-dimethyl sulfoxide (DMSO) and filtered (10-kDa molecular weight cutoff [MWCO]) at 14,000 $\times g$ for 15 min for analysis on a Thermo QExactive Plus with Ultimate 3000 nLC. Peptides were separated on an Accucore C₄ column (15 cm by 75 μ m, 2.6 μ m) at 50°C. Gradient elution (A, 0.2% HCOOH in 95:5 H₂O-DMSO; B, 0.2% HCOOH in 85:10:5 ACN-H₂O-DMSO) was applied: 0 to 1.5 min at 60% B, 35 to 45 min at 96% B, and 45.1 to 60 min at 60% B. Cations generated at 2.2 kV (Nanospray Flex Ion Source) were measured in full MS/ddMS2 mode. The MS1 settings were as follows: m/z = 350 to 1,500, R = 70,000 (full width at half maximum [FWHM]), automatic gain control (AGC) target = 1×10^6 , ITmax = 200 ms. The top 15 precursors with an isolation width of m/z = 2 (z = 2 to 6) underwent high-energy collisional dissociation (HCD) fragmentation at 28% normalized collisional energy (NCE) (N2). MS2 spectra were monitored at the following settings: R = 17.5k, AGC target = 2×10^5 , and maximum number of allowed iterations (ITmax) = 150 ms. Spectra were searched against the *Candida* Genome Database of *C. albicans* SC5314 (10 October 2021) using Proteome Discoverer 2.4 with Sequest HT. FASTA files were manually modified in case of alternative *ECE1* alleles. Both nonspecific and tryptic cleavages with dynamic Met oxidation were considered using precursor and fragment mass tolerances of 10 ppm and 0.02 Da, respectively. Target Decoy PSM Validator was used for q value validation of peptide spectral matches with a false-discovery rate (FDR) of <1%.

Quantification of fungal growth in YPD broth. To analyze total fungal growth of the different fungal strains in YPD medium, a loop of each *C. albicans* strain was grown for 24 h at 37°C in 5 mL of YPD broth under rotation. After incubation, fungal cell suspensions were centrifuged at 3,500 rpm for 5 min and cell pellets were resuspended in 3 mL of PBS and then counted with a Bürker counting chamber.

Quantification of *C. albicans* shedding and growth on vaginal epithelium. The shedding experiments were performed following 2 different protocols for shedding and exfoliation as described here and schematized in Fig. 5A. The shedding protocol was performed according to Graf et al. (54). Briefly, shedding of *C. albicans* strains was measured after 24 h of infection of an A431 monolayer (4×10^5 /mL/well) with the different *C. albicans* clinical isolates (4×10^5 /mL/well). Supernatants were collected and vortexed, whereas cells were treated with 0.2% Triton X-100 to lyse the host cells and release adherent fungal cells. One hundred microliters of supernatants or lysate samples were serially diluted in PBS and seeded in SDA plates. After 48 h of incubation at 37°C, CFU were counted. This protocol allowed us to determine the amount of live *Candida* cells in supernatants, adhered to epithelium and the total fungal growth (Fig. 5A, upper part, shedding protocol). In selected experiments, to analyze the role of type I interferon, the neutralizing anti-human IFNAR2 antibody (4 ng/mL) (PBL InterferonSource) was added to epithelial cells for 3 h before infection as described previously (63).

For the exfoliation protocol, shedding of *C. albicans* strains was measured after 24 h of infection of the A431 monolayer (4×10^5 /mL/well) with the different *C. albicans* clinical isolates (4×10^5 /mL/well). Supernatants were collected by gently pipetting up and down 5 times in each well to recover free fungal cells and fungi attached to or that penetrated the exfoliated epithelial cells. This supernatant was then centrifuged at 1,500 rpm for 5 min with a Microfuge 18 (Beckman Coulter) with an F241.5P rotor and washed twice with warm medium to remove free *Candida* in the supernatant, enriching for exfoliated or shed cells not in suspension. Cellular pellets were then treated with 0.2% Triton X-100 to lyse the shed host cells and release adherent/penetrating fungal cells. Then 100 μ L of each cell suspension was serially diluted in PBS and spread in SDA plates. After 48 h of incubation at 37°C, CFU were counted. Confocal analysis of the exfoliated cell pellet was performed by resuspending the washed pellet (Fig. 5A; dark green) in 100 μ L of PBS plus 1% bovine serum albumin (BSA) without Triton lysis (Fig. 5A; exfoliation protocol). Resuspended pellets were labeled with 20 μ L of Uvitex 2B (1%) in PBS and 5(6)-carboxyfluorescein

diacetate (CDFA) (which labels cytosolic proteins) (1 μ L from a 54.3 μ M stock solution) for 20 min on ice in the dark, washed, and resuspended in 100 μ L of PBS plus 50% glycerol. Slides were imaged using a 63 \times Plan-Apo oil immersion objective mounted on a Leica SP8 confocal microscope equipped with 405-nm and white light lasers. Samples were excited using the 405-nm and 488-nm wavelengths for Uvitex 2B and CFDA, respectively. Mosaic images were acquired using the Navigator tool of LasX software.

Adhesion assay. Yeast cells were suspended in DMEM plus 5% FBS at 4×10^5 /mL. Then 100 μ L of each cell suspension was seeded in triplicate in a 96-well microtiter plate. The plate was incubated for 2 h at 120 rpm and 37°C. After incubation, the wells were washed twice with PBS kept at room temperature to remove unattached yeasts. The adhesion of yeasts was quantified by means of the crystal violet (CV) protocol as previously described (79), with minor modifications. Briefly, 100 μ L of 1% CV was added to each well and allowed to stain for 5 min. The wells were then washed twice with PBS at room temperature. Finally, 100 μ L of 33% acetic acid was added to each well and absorbance was read at 570 nm.

Quantification of *C. albicans*-induced damage of epithelial cells. Lactate dehydrogenase (LDH) release from epithelial cells infected with *Candida* strains was measured after 24 h of infection of the A431 monolayer (4×10^5 /mL/well) with the different *Candida* clinical isolates (4×10^5 /mL/well at an MOI of 1:1 or 2×10^6 /mL/well at an MOI of 1:5) by a specific commercially available kit (BioVision) following the manufacturer's instructions. Calculation of the percentage of cytotoxicity was performed as follows:

$$\% \text{ cytotoxicity} = \frac{(\text{test sample} - \text{low control})}{(\text{high control} - \text{low control})} \times 100$$

Determination of cytokine production. IL-1 β production from epithelial cells infected with *Candida* strains was measured after 24 h of infection of the A431 monolayer (4×10^5 /mL/well) with the different *Candida* clinical isolates (2×10^6 /mL/well at an MOI of 1:5) by a specific commercially available enzyme-linked immunosorbent assay (ELISA) kit (Thermo Fisher) following the manufacturer's instructions.

RNA sequencing and analysis. For the RNA-seq analysis, a monolayer of A431 vaginal cells was infected with *C. albicans* CA01887 and CA14314 (MOI of 1:1) as described above. After 24 h of incubation at 37°C and 5% CO₂, samples were collected in Eppendorf tubes and centrifuged at 3,500 rpm for 5 min. After centrifugation, supernatants were discarded and cell pellets were frozen at -80°C before shipment on dry ice. RNA preparation and next-generation sequencing (NGS) analysis were performed using a protocol based on the NEBNext Ultra II Directional RNA library prep kit (Illumina) and sequencing on a NovaSeq6000 (Illumina) at Eurofins (Eurofins, LLC). The RNA library preparation includes purification of poly(A)-containing mRNA molecules, mRNA fragmentation, random-primed cDNA synthesis (strand specific), Adapter ligation and adapter-specific PCR amplification. Using Galaxy (80), paired-end FASTQ files were analyzed for quality using FastQC and MultiQC (81). All experiments yielded reads that were of high quality according to FastQC, with *Candida*-epithelial cell mixtures having the expected lower GC content due to lower GC in fungal genes. The paired-end reads were trimmed with Trimmomatic (82) and then aligned to the human GRCh38 assembly using HISAT2 (83) in Galaxy. Next, read counts per gene in each sample were generated using HTSeq (84) and Ensembl (85) version 103 annotation of GRCh38 in Galaxy. Read counts per gene were analyzed using R/DESeq2 (86) to examine the correlation of read counts per gene across samples and test for differentially expressed genes. Genes expressed at a low level (those with fewer than 10 mapped reads across all samples) were removed from the analysis. Read counts of genes for duplicate samples were highly correlated by principal-component analysis. Next, levels of gene expression among duplicates of the CA01887 infection were compared to duplicates of uninfected epithelial cells; the same was done for the CA14314 infection, using R/DESeq2 and a false-discovery rate (FDR) of <0.01 . The complete set of results from the R/DESeq2 analyses is available in Data Set S5 and Data Set S6. A total of 1,537 genes were differentially expressed with CA01887 infection and 1,234 genes with CA14314 infection. The two lists of differentially expressed genes, including the corresponding fold change and FDR for those genes, were analyzed using Ingenuity Pathway Analysis (Qiagen). A core analysis was performed, followed by a comparative analysis of canonical pathways. A full list of IPA-identified pathways is presented as Fig. S3 and is shown in Data Set S3. Differentially expressed genes were also analyzed for enriched GO biological process terms using PantherDB GO-Slim Biological Process Overrepresentation Analysis, and DAVID GO Biological Process FAT terms Enrichment Analysis (87–89). An FDR of <0.01 was used to create the list of differentially expressed genes from the R/DESeq2 results for comparisons of infected with CA01887 or CA14314 versus uninfected. An FDR of <0.05 was used for comparisons of CA01887 infected to CA14314 infected. For display of fold change of DESeq2 data in Fig. 6, any differences that were not statistically significant are shown in white, while up-regulated genes are in yellow and downregulated genes are in blue. Data were plotted as log₂ fold change with tools available at <http://www.heatmapper.ca/expression/>.

Statistical analysis. Statistical analyses were performed with GraphPad 8 (Prism). Quantitative variables were tested for normal distribution by Shapiro-Wilk test. Statistical differences between groups were assessed by the two-tailed Student's *t* test and one-way analysis of variance (ANOVA) followed by Tukey's multiple-comparison test or by the nonparametric Mann-Whitney U test and Kruskal-Wallis test, followed by Dunn's multiple-comparison test. The specific test used for each comparison is detailed in the corresponding figure legend. A *P* value of <0.05 was considered significant. Significance throughout the figures is indicated as follows: *, *P* < 0.05; **, *P* < 0.01; and ***, *P* < 0.001.

Data availability. Gene expression data and sequence data are accessible at the NCBI Gene Expression Omnibus under accession no. GSE207081.

SUPPLEMENTAL MATERIAL

Supplemental material is available online only.

FIG S1, PDF file, 0.6 MB.

FIG S2, PDF file, 0.5 MB.

FIG S3, TIF file, 7 MB.

DATA SET S1, XLSX file, 0.1 MB.

DATA SET S2, XLSX file, 0.02 MB.

DATA SET S3, XLSX file, 0.1 MB.

DATA SET S4, XLSX file, 1.3 MB.

DATA SET S5, XLSX file, 6.6 MB.

DATA SET S6, XLSX file, 6.6 MB.

ACKNOWLEDGMENTS

The Leica SP8 confocal microscope is available at the imaging facility (Centro Interdipartimentale Grandi Strumenti [CIGS]) of the University of Modena and Reggio Emilia. We thank Jonathan Vinet from CIGS for technical support and James H. Wheeler for work on CL allele cloning. We thank Giuseppina Campisciano for her collaboration in the collection, storage, and shipping of *Candida* strains obtained from IRCCS Burlo Garofolo of Trieste.

B.L.K. was funded by Institutional Development Award (IDeA) from the National Institute of General Medical Sciences of the National Institutes of Health under grant no. P20GM103423. This work was supported by the Deutsche Forschungsgemeinschaft (DFG)-funded Collaborative Research Center/Transregio 124 FungiNet (project no. 210879364, project Z2 to O.K.). R.T.W. was funded by NIH (R15AI133415), the Investigator in the Pathogenesis of Infectious Disease grant from the Burroughs Wellcome Fund, and the USDA National Institute of Food and Agriculture, Hatch project no. ME0-21821. E.P. was funded by FAR Mission Oriented 2022 and by FAR departmental 2022 instrumentation line.

REFERENCES

- Ardizzone A, Wheeler RT, Pericolini E. 2021. It takes two to tango: how a dysregulation of the innate immunity, coupled with *Candida* virulence, triggers VVC onset. *Front Microbiol* 12:692491. <https://doi.org/10.3389/fmicb.2021.692491>.
- Kalia N, Singh J, Kaur M. 2020. Microbiota in vaginal health and pathogenesis of recurrent vulvovaginal infections: a critical review. *Ann Clin Microbiol Antimicrob* 19:5. <https://doi.org/10.1186/s12941-020-0347-4>.
- Cassone A. 2015. Vulvovaginal *Candida albicans* infections: pathogenesis, immunity and vaccine prospects. *BJOG* 122:785–794. <https://doi.org/10.1111/1471-0528.12994>.
- Sobel JD, Faro S, Force RW, Foxman B, Ledger WJ, Nyirjesy PR, Reed BD, Summers PR. 1998. Vulvovaginal candidiasis: epidemiologic, diagnostic, and therapeutic considerations. *Am J Obstet Gynecol* 178:203–211. [https://doi.org/10.1016/s0002-9378\(98\)80001-x](https://doi.org/10.1016/s0002-9378(98)80001-x).
- Blostein F, Levin-Sparenberg E, Wagner J, Foxman B. 2017. Recurrent vulvovaginal candidiasis. *Ann Epidemiol* 27:575–582.e3. <https://doi.org/10.1016/j.annepidem.2017.08.010>.
- Denning DW, Kneale M, Sobel JD, Rautemaa-Richardson R. 2018. Global burden of recurrent vulvovaginal candidiasis: a systematic review. *Lancet Infect Dis* 18:e339–e347. [https://doi.org/10.1016/S1473-3099\(18\)30103-8](https://doi.org/10.1016/S1473-3099(18)30103-8).
- Goncalves B, Ferreira C, Alves CT, Henriques M, Azeredo J, Silva S. 2016. Vulvovaginal candidiasis: epidemiology, microbiology and risk factors. *Crit Rev Microbiol* 42:905–927. <https://doi.org/10.3109/1040841X.2015.1091805>.
- Perslev K, Msemu OA, Minja DTR, Moller SL, Theander TG, Lusingu JPA, Bygbjerg IC, Nielsen BB, Schmiedel C. 2019. Marked reduction in fertility among African women with urogenital infections: a prospective cohort study. *PLoS One* 14:e0210421. <https://doi.org/10.1371/journal.pone.0210421>.
- Jaeger M, Carvalho A, Cunha C, Plantinga TS, van de Veerdonk F, Puccetti M, Galosi C, Joosten LA, Dupont B, Kullberg BJ, Sobel JD, Romani L, Netea MG. 2016. Association of a variable number tandem repeat in the NLRP3 gene in women with susceptibility to RVVC. *Eur J Clin Microbiol Infect Dis* 35:797–801. <https://doi.org/10.1007/s10096-016-2600-5>.
- Jaeger M, Pinelli M, Borghi M, Constantini C, Dindo M, van Emst L, Puccetti M, Pariano M, Ricano-Ponce I, Bull C, Gresnigt MS, Wang X, Gutierrez Achury J, Jacobs CWM, Xu N, Oosting M, Arts P, Joosten LAB, van de Veerdonk FL, Veltman JA, Ten Oever J, Kullberg BJ, Feng M, Adema GJ, Wijmenga C, Kumar V, Sobel J, Gilissen C, Romani L, Netea MG. 2019. A systems genomics approach identifies SIGLEC15 as a susceptibility factor in recurrent vulvovaginal candidiasis. *Sci Transl Med* 11:eaar3558. <https://doi.org/10.1126/scitranslmed.aar3558>.
- Jaeger M, van der Lee R, Cheng SC, Johnson MD, Kumar V, Ng A, Plantinga TS, Smeekens SP, Oosting M, Wang X, Barchet W, Fitzgerald K, Joosten LAB, Perfect JR, Wijmenga C, van de Veerdonk FL, Huynen MA, Xavier RJ, Kullberg BJ, Netea MG. 2015. The RIG-I-like helicase receptor MDA5 (IFIH1) is involved in the host defense against *Candida* infections. *Eur J Clin Microbiol Infect Dis* 34:963–974. <https://doi.org/10.1007/s10096-014-2309-2>.
- Willems HME, Ahmed SS, Liu J, Xu Z, Peters BM. 2020. Vulvovaginal candidiasis: a current understanding and burning questions. *J Fungi (Basel)* 6:27. <https://doi.org/10.3390/jof6010027>.
- Jabra-Rizk MA, Kong EF, Tsui C, Nguyen MH, Clancy CJ, Fidel PL, Jr, Noverr M. 2016. *Candida albicans* pathogenesis: fitting within the host-microbe damage response framework. *Infect Immun* 84:2724–2739. <https://doi.org/10.1128/IAI.00469-16>.
- Kumwenda P, Cottier F, Hendry AC, Kneafsey D, Keevan B, Gallagher H, Tsai HJ, Hall RA. 2022. Estrogen promotes innate immune evasion of *Candida albicans* through inactivation of the alternative complement system. *Cell Rep* 38:110183. <https://doi.org/10.1016/j.celrep.2021.110183>.
- Naglik JR, Richardson JP, Moyes DL. 2014. *Candida albicans* pathogenicity and epithelial immunity. *PLoS Pathog* 10:e1004257. <https://doi.org/10.1371/journal.ppat.1004257>.
- Yano J, Peters BM, Noverr MC, Fidel PL, Jr. 2018. Novel mechanism behind the immunopathogenesis of vulvovaginal candidiasis: neutrophil anergy. *Infect Immun* 86:e00684-17. <https://doi.org/10.1128/IAI.00684-17>.
- Liu Y, Shetty AC, Schwartz JA, Bradford LL, Xu W, Phan QT, Kumari P, Mahurkar A, Mitchell AP, Ravel J, Fraser CM, Filler SG, Bruno VM. 2015. New signaling pathways govern the host response to *C. albicans* infection in various niches. *Genome Res* 25:679–689. <https://doi.org/10.1101/gr.187427.114>.

18. Pekmezovic M, Mogavero S, Naglik JR, Hube B. 2019. Host-pathogen interactions during female genital tract infections. *Trends Microbiol* 27: 982–996. <https://doi.org/10.1016/j.tim.2019.07.006>.
19. Pericolini E, Perito S, Castagnoli A, Gabrielli E, Mencacci A, Blasi E, Vecchiarelli A, Wheeler RT. 2018. Epitope unmasking in vulvovaginal candidiasis is associated with hyphal growth and neutrophilic infiltration. *PLoS One* 13:e0201436. <https://doi.org/10.1371/journal.pone.0201436>.
20. Marakalala MJ, Vautier S, Potrykus J, Walker LA, Shepardson KM, Hopke A, Mora-Montes HM, Kerrigan A, Netea MG, Murray GI, MacCallum DM, Wheeler R, Munro CA, Gow NA, Cramer RA, Brown AJ, Brown GD. 2013. Differential adaptation of *Candida albicans* in vivo modulates immune recognition by dectin-1. *PLoS Pathog* 9:e1003315. <https://doi.org/10.1371/journal.ppat.1003315>.
21. Bertolini M, Ranjan A, Thompson A, Diaz PI, Sobue T, Maas K, Dongari-Bagtzoglou A. 2019. *Candida albicans* induces mucosal bacterial dysbiosis that promotes invasive infection. *PLoS Pathog* 15:e1007717. <https://doi.org/10.1371/journal.ppat.1007717>.
22. Li XV, Leonardi I, Putzel GG, Semon A, Fiers WD, Kusakabe T, Lin WY, Gao IH, Doron I, Gutierrez-Guerrero A, DeCelle MB, Carriche GM, Mesko M, Yang C, Naglik JR, Hube B, Scherl EJ, Iliev ID. 2022. Immune regulation by fungal strain diversity in inflammatory bowel disease. *Nature* 603:672–678. <https://doi.org/10.1038/s41586-022-04502-w>.
23. Mason KL, Erb Downward JR, Falkowski NR, Young VB, Kao JY, Huffnagle GB. 2012. Interplay between the gastric bacterial microbiota and *Candida albicans* during postantibiotic recolonization and gastritis. *Infect Immun* 80:150–158. <https://doi.org/10.1128/IAI.05162-11>.
24. Break TJ, Jaeger M, Solis NV, Filler SG, Rodriguez CA, Lim JK, Lee CC, Sobel JD, Netea MG, Lionakis MS. 2015. CX3CR1 is dispensable for control of mucosal *Candida albicans* infections in mice and humans. *Infect Immun* 83:958–965. <https://doi.org/10.1128/IAI.02604-14>.
25. Schonherr FA, Sparber F, Kirchner FR, Guiducci E, Trautwein-Weidner K, Gladiator A, Sertour N, Hetzel U, Le GTT, Pavelka N, d'Enfert C, Bougnoux ME, Corti CF, LeibundGut-Landmann S. 2017. The intraspecies diversity of *C. albicans* triggers qualitatively and temporally distinct host responses that determine the balance between commensalism and pathogenicity. *Mucosal Immunol* 10:1335–1350. <https://doi.org/10.1038/mi.2017.2>.
26. Liu J, Willems HME, Sansever EA, Allert S, Barker KS, Lowes DJ, Dixon AC, Xu Z, Miao J, DeJarnette C, Tournu H, Palmer GE, Richardson JP, Barrera FN, Hube B, Naglik JR, Peters BM. 2021. A variant ECE1 allele contributes to reduced pathogenicity of *Candida albicans* during vulvovaginal candidiasis. *PLoS Pathog* 17:e1009884. <https://doi.org/10.1371/journal.ppat.1009884>.
27. Willems HME, Lowes DJ, Barker KS, Palmer GE, Peters BM. 2018. Comparative analysis of the capacity of the *Candida* species to elicit vaginal immunopathology. *Infect Immun* 86:e00527-18. <https://doi.org/10.1128/IAI.00527-18>.
28. Gerwien F, Dunker C, Brandt P, Garbe E, Jacobsen ID, Vylkova S. 2020. Clinical *Candida albicans* vaginal isolates and a laboratory strain show divergent behaviors during macrophage interactions. *mSphere* 5:e00393-20. <https://doi.org/10.1128/mSphere.00393-20>.
29. Li C, Wang L, Tong H, Ge Y, Mei H, Chen L, Lv G, Liu W. 2016. Microsatellite analysis of genotype distribution patterns of *Candida albicans* vulvovaginal candidiasis in Nanjing, China and its association with pregnancy, age and clinical presentation. *Arch Gynecol Obstet* 294:291–297. <https://doi.org/10.1007/s00404-016-4029-6>.
30. Monroy-Perez E, Paniagua-Contreras GL, Rodriguez-Purata P, Vaca-Paniagua F, Vazquez-Villasenor M, Diaz-Velasquez C, Uribe-Garcia A, Vaca S. 2016. High virulence and antifungal resistance in clinical strains of *Candida albicans*. *Can J Infect Dis Med Microbiol* 2016:5930489. <https://doi.org/10.1155/2016/5930489>.
31. Wang M, Cao Y, Xia M, Al-Hatmi AM, Ou W, Wang Y, Sibiry AA, Zhao L, Zou C, Liao W, Bai F, Zhi X, Hoog S, Kang Y. 2019. Virulence and antifungal susceptibility of microsatellite genotypes of *Candida albicans* from superficial and deep locations. *Yeast* 36:363–373. <https://doi.org/10.1002/yea.3397>.
32. Ying C, Zhang H, Tang Z, Chen H, Gao J, Yue C. 2016. Antifungal susceptibility and molecular typing of 115 *Candida albicans* isolates obtained from vulvovaginal candidiasis patients in 3 Shanghai maternity hospitals. *Med Mycol* 54:394–399. <https://doi.org/10.1093/mmy/myv082>.
33. Bruno VM, Shetty AC, Yano J, Fidel PL, Jr, Noverr MC, Peters BM. 2015. Transcriptomic analysis of vulvovaginal candidiasis identifies a role for the NLRP3 inflammasome. *mBio* 6:e00182-15. <https://doi.org/10.1128/mBio.00182-15>.
34. Pericolini E, Gabrielli E, Amacker M, Kasper L, Roselletti E, Luciano E, Sabbatini S, Kaeser M, Moser C, Hube B, Vecchiarelli A, Cassone A. 2015. Secretory aspartyl proteinases cause vaginitis and can mediate vaginitis caused by *Candida albicans* in mice. *mBio* 6:e00724-15. <https://doi.org/10.1128/mBio.00724-15>.
35. Peters BM, Palmer GE, Nash AK, Lilly EA, Fidel PL, Jr, Noverr MC. 2014. Fungal morphogenetic pathways are required for the hallmark inflammatory response during *Candida albicans* vaginitis. *Infect Immun* 82:532–543. <https://doi.org/10.1128/IAI.01417-13>.
36. Richardson JP, Willems HME, Moyes DL, Shoaie S, Barker KS, Tan SL, Palmer GE, Hube B, Naglik JR, Peters BM. 2018. Candidalysin drives epithelial signaling, neutrophil recruitment, and immunopathology at the vaginal mucosa. *Infect Immun* 86:e00645-17. <https://doi.org/10.1128/IAI.00645-17>.
37. Moyes DL, Wilson D, Richardson JP, Mogavero S, Tang SX, Wernecke J, Hofs S, Gratacap RL, Robbins J, Runglall M, Murciano C, Blagojevic M, Thavaraj S, Forster TM, Hebecker B, Kasper L, Vizcay G, Iancu SI, Kichik N, Hader A, Kurzai O, Luo T, Kruger T, Kniemeyer O, Cota E, Bader O, Wheeler RT, Gutschmann T, Hube B, Naglik JR. 2016. Candidalysin is a fungal peptide toxin critical for mucosal infection. *Nature* 532:64–68. <https://doi.org/10.1038/nature17625>.
38. Roselletti E, Monari C, Sabbatini S, Perito S, Vecchiarelli A, Sobel JD, Cassone A. 2019. A role for yeast/pseudohyphal cells of *Candida albicans* in the correlated expression of NLRP3 inflammasome inducers in women with acute vulvovaginal candidiasis. *Front Microbiol* 10:2669. <https://doi.org/10.3389/fmicb.2019.02669>.
39. Roselletti E, Perito S, Sabbatini S, Monari C, Vecchiarelli A. 2019. Vaginal epithelial cells discriminate between yeast and hyphae of *Candida albicans* in women who are colonized or have vaginal candidiasis. *J Infect Dis* 220:1645–1654. <https://doi.org/10.1093/infdis/jiz365>.
40. de Barros PP, Scorzoni L, Ribeiro FC, Fugisaki LRO, Fuchs BB, Mylonakis E, Jorge AOC, Junqueira JC, Rossoni RD. 2018. *Lactobacillus paracasei* 28.4 reduces in vitro hyphae formation of *Candida albicans* and prevents the filamentation in an experimental model of *Caenorhabditis elegans*. *Microb Pathog* 117:80–87. <https://doi.org/10.1016/j.micpath.2018.02.019>.
41. Jang SJ, Lee K, Kwon B, You HJ, Ko G. 2019. Vaginal lactobacilli inhibit growth and hyphae formation of *Candida albicans*. *Sci Rep* 9:8121. <https://doi.org/10.1038/s41598-019-44579-4>.
42. Orsi CF, Sabia C, Ardizzoni A, Colombari B, Neglia RG, Peppoloni S, Morace G, Blasi E. 2014. Inhibitory effects of different lactobacilli on *Candida albicans* hyphal formation and biofilm development. *J Biol Regul Homeost Agents* 28:743–752.
43. Barousse MM, Steele C, Dunlap K, Espinosa T, Boikov D, Sobel JD, Fidel PL, Jr. 2001. Growth inhibition of *Candida albicans* by human vaginal epithelial cells. *J Infect Dis* 184:1489–1493. <https://doi.org/10.1086/324532>.
44. Ardizzoni A, Sala A, Colombari B, Giva LB, Cermelli C, Peppoloni S, Vecchiarelli A, Roselletti E, Blasi E, Wheeler RT, Pericolini E. 2020. Perinuclear anti-neutrophil cytoplasmic antibodies (pANCA) impair neutrophil candidicidal activity and are increased in the cellular fraction of vaginal samples from women with vulvovaginal candidiasis. *J Fungi (Basel)* 6:225. <https://doi.org/10.3390/jof6040225>.
45. Fidel PL, Jr, Barousse M, Espinosa T, Ficarra M, Sturtevant J, Martin DH, Quayle AJ, Dunlap K. 2004. An intravaginal live *Candida* challenge in humans leads to new hypotheses for the immunopathogenesis of vulvovaginal candidiasis. *Infect Immun* 72:2939–2946. <https://doi.org/10.1128/IAI.72.5.2939-2946.2004>.
46. Moyes DL, Murciano C, Runglall M, Islam A, Thavaraj S, Naglik JR. 2011. *Candida albicans* yeast and hyphae are discriminated by MAPK signaling in vaginal epithelial cells. *PLoS One* 6:e26580. <https://doi.org/10.1371/journal.pone.0026580>.
47. Bishop GB. 1990. Chapter 172. Vaginal discharge. In Walker HK, Hall WD, Hurst JW (ed), *Clinical methods: the history, physical, and laboratory examinations*, 3rd ed. Butterworths, Boston, MA.
48. O'Hanlon DE, Brown SE, He X, Stennett CA, Robbins SJ, Johnston ED, Wnorowski AM, Mark K, Ravel J, Cone RA, Brotman RM. 2021. Observational cohort study of the effect of a single lubricant exposure during transvaginal ultrasound on cell-shedding from the vaginal epithelium. *PLoS One* 16:e0250153. <https://doi.org/10.1371/journal.pone.0250153>.
49. O'Hanlon DE, Gajer P, Brotman RM, Ravel J. 2020. Asymptomatic bacterial vaginosis is associated with depletion of mature superficial cells shed from the vaginal epithelium. *Front Cell Infect Microbiol* 10:106. <https://doi.org/10.3389/fcimb.2020.00106>.
50. Amegashie CP, Gilbert NM, Peipert JF, Allsworth JE, Lewis WG, Lewis AL. 2017. Relationship between Nugent score and vaginal epithelial exfoliation. *PLoS One* 12:e0177797. <https://doi.org/10.1371/journal.pone.0177797>.
51. Knodler LA, Vallance BA, Celli J, Winfree S, Hansen B, Montero M, Steele-Mortimer O. 2010. Dissemination of invasive *Salmonella* via bacterial-induced extrusion of mucosal epithelia. *Proc Natl Acad Sci U S A* 107: 17733–17738. <https://doi.org/10.1073/pnas.1006098107>.

52. Muenzner P, Hauck CR. 2020. Neisseria gonorrhoeae blocks epithelial exfoliation by nitric-oxide-mediated metabolic cross talk to promote colonization in mice. *Cell Host Microbe* 27:793–808.e5. <https://doi.org/10.1016/j.chom.2020.03.010>.
53. Vornhagen J, Armistead B, Santana-Ufret V, Gendrin C, Merillat S, Coleman M, Quach P, Boldenow E, Alishetti V, Leonhard-Melief C, Ngo LY, Whidbey C, Doran KS, Curtis C, Waldorf KMA, Nance E, Rajagopal L. 2018. Group B streptococcus exploits vaginal epithelial exfoliation for ascending infection. *J Clin Invest* 128:1985–1999. <https://doi.org/10.1172/JCI97043>.
54. Graf K, Last A, Gratz R, Allert S, Linde S, Westermann M, Groger M, Mosig AS, Gresnigt MS, Hube B. 2019. Keeping *Candida* commensal: how lactobacilli antagonize pathogenicity of *Candida albicans* in an in vitro gut model. *Dis Model Mech* 12:dmm039719. <https://doi.org/10.1242/dmm.039719>.
55. Amaral EP, Costa DL, Namasivayam S, Riteau N, Kamenyeva O, Mittereder L, Mayer-Barber KD, Andrade BB, Sher A. 2019. A major role for ferroptosis in Mycobacterium tuberculosis-induced cell death and tissue necrosis. *J Exp Med* 216:556–570. <https://doi.org/10.1084/jem.20181776>.
56. Gazendam RP, van Hamme JL, Tool AT, van Houdt M, Verkuijlen PJ, Herbst M, Liese JG, van de Veerdonk FL, Roos D, van den Berg TK, Kuijpers TW. 2014. Two independent killing mechanisms of *Candida albicans* by human neutrophils: evidence from innate immunity defects. *Blood* 124:590–597. <https://doi.org/10.1182/blood-2014-01-551473>.
57. Jawhara S, Pluskota E, Verbovetskiy D, Skomorovska-Prokvolit O, Plow EF, Soloviev DA. 2012. Integrin alphaXbeta(2) is a leukocyte receptor for *Candida albicans* and is essential for protection against fungal infections. *J Immunol* 189:2468–2477. <https://doi.org/10.4049/jimmunol.1200524>.
58. Johnson CM, O'Brien XM, Byrd AS, Parisi VE, Loosely AJ, Li W, Witt H, Faridi HM, Lefort CT, Gupta V, Kim M, Reichner JS. 2017. Integrin cross-talk regulates the human neutrophil response to fungal beta-glucan in the context of the extracellular matrix: a prominent role for VLA3 in the antifungal response. *J Immunol* 198:318–334. <https://doi.org/10.4049/jimmunol.1502381>.
59. Mao H, Zhao Y, Li H, Lei L. 2020. Ferroptosis as an emerging target in inflammatory diseases. *Prog Biophys Mol Biol* 155:20–28. <https://doi.org/10.1016/j.pbiomolbio.2020.04.001>.
60. O'Brien XM, Reichner JS. 2016. Neutrophil integrins and matrix ligands and NET release. *Front Immunol* 7:363. <https://doi.org/10.3389/fimmu.2016.00363>.
61. Soloviev DA, Fonzi WA, Sentandreu R, Pluskota E, Forsyth CB, Yadav S, Plow EF. 2007. Identification of pH-regulated antigen 1 released from *Candida albicans* as the major ligand for leukocyte integrin alphaXbeta2. *J Immunol* 178:2038–2046. <https://doi.org/10.4049/jimmunol.178.4.2038>.
62. Stockwell BR, Jiang X. 2020. The chemistry and biology of ferroptosis. *Cell Chem Biol* 27:365–375. <https://doi.org/10.1016/j.chembiol.2020.03.013>.
63. Pekmezovic M, Hovhannisyann H, Gresnigt MS, Iracane E, Oliveira-Pacheco J, Siscar-Lewin S, Seemann E, Qualmann B, Kalkreuter T, Muller S, Kamradt T, Mogavero S, Brunke S, Butler G, Gabaldon T, Hube B. 2021. *Candida* pathogens induce protective mitochondria-associated type I interferon signalling and a damage-driven response in vaginal epithelial cells. *Nat Microbiol* 6:643–657. <https://doi.org/10.1038/s41564-021-00875-2>.
64. Kolben T, Pieper K, Goess C, Degenhardt T, Ditsch N, Weissenbacher T, Weissenbacher ER, Kolben TM. 2017. IL-23, IFN-alpha, and IFN-beta in the vaginal fluid of patients suffering from vulvovaginal candidosis. *Clin Exp Obstet Gynecol* 44:7–10. <https://doi.org/10.12891/ceog3391.2017>.
65. Li T, Liu Z, Zhang X, Chen X, Wang S. 2019. Therapeutic effectiveness of type I interferon in vulvovaginal candidiasis. *Microb Pathog* 134:103562. <https://doi.org/10.1016/j.micpath.2019.103562>.
66. Mogavero S, Sauer FM, Brunke S, Allert S, Schulz D, Wisgott S, Jablonowski N, Elshafie O, Kruger T, Kniemeyer O, Brakhage AA, Naglik JR, Dolk E, Hube B. 2021. Candidalysin delivery to the invasion pocket is critical for host epithelial damage induced by *Candida albicans*. *Cell Microbiol* 23:e13378. <https://doi.org/10.1111/cmi.13378>.
67. Hostetter MK. 1999. Integrin-like proteins in *Candida* spp. and other microorganisms. *Fungal Genet Biol* 28:135–145. <https://doi.org/10.1006/fgbi.1999.1165>.
68. Puri S, Kumar R, Rojas IG, Salvatori O, Edgerton M. 2019. Iron chelator deferasirox reduces *Candida albicans* invasion of oral epithelial cells and infection levels in murine oropharyngeal candidiasis. *Antimicrob Agents Chemother* 63:e02152–18. <https://doi.org/10.1128/AAC.02152-18>.
69. Savage KA, Parquet MC, Allan DS, Davidson RJ, Holbein BE, Lilly EA, Fidel PL, Jr. 2018. Iron restriction to clinical isolates of *Candida albicans* by the novel chelator DIBI inhibits growth and increases sensitivity to azoles in vitro and in vivo in a murine model of experimental vaginitis. *Antimicrob Agents Chemother* 62:e02576–17. <https://doi.org/10.1128/AAC.02576-17>.
70. Millet N, Solis NV, Aguilar D, Lionakis MS, Wheeler RT, Jendzjowsky N, Swidergall M. 2022. IL-23 signaling prevents ferroptosis-driven renal immunopathology during candidiasis. *Nat Commun* 13:5545. <https://doi.org/10.1038/s41467-022-33327-4>.
71. Nyirjesy P, Brookhart C, Lazenby G, Schwebke J, Sobel JD. 2022. Vulvovaginal candidiasis: a review of the evidence for the 2021 Centers for Disease Control and Prevention of Sexually Transmitted Infections Treatment Guidelines. *Clin Infect Dis* 74(Suppl 2):S162–S168. <https://doi.org/10.1093/cid/ciab1057>.
72. Bounoux ME, Tavanti A, Bouchier C, Gow NA, Magnier A, Davidson AD, Maiden MC, D'Enfert C, Odds FC. 2003. Collaborative consensus for optimized multilocus sequence typing of *Candida albicans*. *J Clin Microbiol* 41:5265–5266. <https://doi.org/10.1128/JCM.41.11.5265-5266.2003>.
73. Tavanti A, Davidson AD, Fordyce MJ, Gow NA, Maiden MC, Odds FC. 2005. Population structure and properties of *Candida albicans*, as determined by multilocus sequence typing. *J Clin Microbiol* 43:5601–5613. <https://doi.org/10.1128/JCM.43.11.5601-5613.2005>.
74. Tavanti A, Gow NA, Senesi S, Maiden MC, Odds FC. 2003. Optimization and validation of multilocus sequence typing for *Candida albicans*. *J Clin Microbiol* 41:3765–3776. <https://doi.org/10.1128/JCM.41.8.3765-3776.2003>.
75. Kumar S, Tamura K, Jakobsen IB, Nei M. 2001. MEGA2: Molecular Evolutionary Genetics Analysis software. *Bioinformatics* 17:1244–1245. <https://doi.org/10.1093/bioinformatics/17.12.1244>.
76. Hoffman CS, Winston F. 1987. A ten-minute DNA preparation from yeast efficiently releases autonomous plasmids for transformation of *Escherichia coli*. *Gene* 57:267–272. [https://doi.org/10.1016/0378-1119\(87\)90131-4](https://doi.org/10.1016/0378-1119(87)90131-4).
77. Sievers F, Willm A, Dineen D, Gibson TJ, Karplus K, Li W, Lopez R, McWilliam H, Remmert M, Soding J, Thompson JD, Higgins DG. 2011. Fast, scalable generation of high-quality protein multiple sequence alignments using Clustal Omega. *Mol Syst Biol* 7:539. <https://doi.org/10.1038/msb.2011.75>.
78. Kimura M. 1980. A simple method for estimating evolutionary rates of base substitutions through comparative studies of nucleotide sequences. *J Mol Evol* 16:111–120. <https://doi.org/10.1007/BF01731581>.
79. Negri M, Goncalves V, Silva S, Henriques M, Azeredo J, Oliveira R. 2010. Crystal violet staining to quantify *Candida* adhesion to epithelial cells. *Br J Biomed Sci* 67:120–125. <https://doi.org/10.1080/09674845.2010.11730308>.
80. Galaxy Community. 2022. The Galaxy platform for accessible, reproducible and collaborative biomedical analyses: 2022 update. *Nucleic Acids Res* 50:W345–W351. <https://doi.org/10.1093/nar/gkac247>.
81. Ewels P, Magnusson M, Lundin S, Kaller M. 2016. MultiQC: summarize analysis results for multiple tools and samples in a single report. *Bioinformatics* 32:3047–3048. <https://doi.org/10.1093/bioinformatics/btw354>.
82. Bolger AM, Lohse M, Usadel B. 2014. Trimmomatic: a flexible trimmer for Illumina sequence data. *Bioinformatics* 30:2114–2120. <https://doi.org/10.1093/bioinformatics/btu170>.
83. Kim D, Langmead B, Salzberg SL. 2015. HISAT: a fast spliced aligner with low memory requirements. *Nat Methods* 12:357–360. <https://doi.org/10.1038/nmeth.3317>.
84. Anders S, Pyl PT, Huber W. 2015. HTSeq—a Python framework to work with high-throughput sequencing data. *Bioinformatics* 31:166–169. <https://doi.org/10.1093/bioinformatics/btu638>.
85. Yates AD, Achuthan P, Akanni W, Allen J, Allen J, Alvarez-Jarreta J, Amode MR, Armean IM, Azov AG, Bennett R, Bhai J, Billis K, Boddus S, Marugán JC, Cummins C, Davidson C, Dodiya K, Fatima R, Gall A, Giron CG, Gil L, Grego T, Haggerty L, Haskell E, Hourlier T, Izuogu OG, Janacek SH, Juettemann T, Kay M, Lavidas I, Le T, Lemos D, Martinez JG, Maurel T, McDowall M, McMahon A, Mohanan S, Moore B, Nuhn M, Ohed DN, Parker A, Parton A, Patricio M, Sakthivel MP, Abdul Salam AI, Schmitt BM, Schuilenburg H, Sheppard D, Sycheva M, Szuba M, et al. 2020. Ensembl 2020. *Nucleic Acids Res* 48:D682–D688. <https://doi.org/10.1093/nar/gkz966>.
86. Love MI, Huber W, Anders S. 2014. Moderated estimation of fold change and dispersion for RNA-seq data with DESeq2. *Genome Biol* 15:550. <https://doi.org/10.1186/s13059-014-0550-8>.
87. Mi H, Muruganujan A, Huang X, Ebert D, Mills C, Guo X, Thomas PD. 2019. Protocol update for large-scale genome and gene function analysis with the PANTHER classification system (v.14.0). *Nat Protoc* 14:703–721. <https://doi.org/10.1038/s41596-019-0128-8>.
88. Sherman BT, Hao M, Qiu J, Jiao X, Baseler MW, Lane HC, Imamichi T, Chang W. 2022. DAVID: a web server for functional enrichment analysis and functional annotation of gene lists (2021 update). *Nucleic Acids Res* 50:W216–W221. <https://doi.org/10.1093/nar/gkac194>.
89. Thomas PD, Ebert D, Muruganujan A, Mushayama T, Albou LP, Mi H. 2022. PANTHER: making genome-scale phylogenetics accessible to all. *Protein Sci* 31:8–22. <https://doi.org/10.1002/pro.4218>.